TASK QUARTERLY 11 No 4, 315–328

TWO-DIMENSIONAL VERTICAL ANALYSIS OF DAM-BREAK FLOW

PIOTR ZIMA

Gdansk University of Technology,
Faculty of Civil and Environmental Engineering,
Narutowicza 11/12, 80-952 Gdansk, Poland
pzim@pg.gda.pl

(Received 15 July 2007)

Abstract: The paper concerns mathematical modeling of free surface open-channel water flow. Two-dimensional vertical Reynolds-averaged Navier-Stokes equations were used to simulate the flow. They were solved with the SIMPLE algorithm of the finite difference method using the Marker and Cell technique to trace free surface movement. The dam-break flow (water column collapse) problem on a horizontal and frictionless bottom was investigated as a test case. The mechanics of dam-break flow for wet and dry bed conditions was analyzed on the basis of numerical simulations. The obtained results are shown for varying head of water in the downstream channel. The possibility of using the shallow-water equations and the RANS model to simulate rapidly varied flows is discussed.

Keywords: mathematical modeling, Reynolds-averaged Navier-Stokes equations, rapidly varied free surface flow, dam-break flow

1. Introduction

During the last few years, the shallow-water equations (SWE) have been successfully applied, in their depth-averaged form, to many engineering problems. Their use has become standard practice in environmental impact studies concerned with flood plain management in river valleys, especially in dam-break flow (DBF) problems [1]. As these models have assumed hydrostatic pressure and uniform velocity distribution along the water depth, they are not adequate descriptions of the flow near local hydraulic effects such as steep wave fronts, hydraulic jumps, *etc.* [2]. Better simulation results for short-term problems can be obtained using a model including non-hydrostatic pressure and variable-depth velocity.

The mathematical equations representing the fundamental laws of physics governing the phenomenon of free surface water flow, the Navier-Stokes (NS) equations, are well known. The vertical Reynolds-Averaged NS (RANS) equations are the most widely used model of two-dimensional flow. The NS equations are a system of partial differential equations describing incompressible viscous flow [3]. Unfortunately, an analytical solution of NS equations does not exist for most real cases, and they

must be solved using numerical methods. There is a number of well-known and successfully applied classical methods of solving water flow equations [4–6]. They are based on the three fundamental methods: the finite difference method (FDM), the finite element method (FEM) and the finite volume method (FVM). One of the most popular and often used procedures is the Semi-Implicit Method for Pressure-Linked Equations (SIMPLE) algorithm [7]. SIMPLE, which is not a specific method, but rather a general approach, is an iterative technique solving RANS equations considering their divergence. It leads to the Poisson equation, which describes pressure field evolution (the pressure-correction equation). In the study presented in this paper, DBF problems (with dry and wet beds) have been considered and their pressure and velocity profiles shown. The SIMPLE method was used to solve two-dimensional vertical RANS equations on a rectangular, staggered grid [8].

When RANS equations are used to describe an open-channel flow, the free surface movement problem must be solved. As a free surface moves with the velocity of the fluid particles located at its boundary, its position must be found during computations. One of the techniques of solving this problem is the Marker and Cell (MAC) method [9]. The application of this method to solve open channel flows is possible but unique due to the huge computational effort required to simulate some real cases. Therefore, its solutions are often limited to two-dimensional cases in the vertical plane [10–12].

2. RANS equations and solution method

The governing equations for incompressible viscous flow are the continuity equation and the RANS equations, which can be written in the following form [3]:

$$\nabla \boldsymbol{u} = 0, \tag{1}$$

$$\frac{D\boldsymbol{u}}{Dt} = \boldsymbol{f} - \frac{1}{\rho}\nabla p + \nu \Delta u, \tag{2}$$

where $\boldsymbol{u}$ represents the velocity vector, $\boldsymbol{f}$ is a vector of external forces, p is pressure, ϱ is density, and ν is the kinetic viscosity factor. If we operate the divergence operator on Equation (2), the pressure-correction equation can be written as [8]:

$$\Delta \bar{p} = -\nabla \cdot (u \cdot \nabla u), \tag{3}$$

where $\bar{p}$ denotes normalized pressure expressed as $\bar{p} = p/\rho$.

RANS are solved in the vertical Cartesian plane x–y (neglecting one of the horizontal dimensions) for two velocity components only (horizontal u_x in the x direction and vertical u_y in the y direction) and for pressure, p. The external body forces' vector includes the acceleration due to gravity, g, with components ϱg. Equations (1)–(3) can be rewritten in their differential form for both velocity components as follows:

$$\frac{\partial u_x}{\partial x} + \frac{\partial u_y}{\partial y} = 0, \tag{4}$$

$$\begin{cases} \dfrac{\partial u_x}{\partial t} + u_x \dfrac{\partial u_x}{\partial x} + u_y \dfrac{\partial u_x}{\partial y} = g_x - \dfrac{1}{\rho}\dfrac{\partial p}{\partial x} + \nu \left(\dfrac{\partial^2 u_x}{\partial x^2} + \dfrac{\partial^2 u_x}{\partial y^2} \right), \\ \dfrac{\partial u_y}{\partial t} + u_x \dfrac{\partial u_y}{\partial x} + u_y \dfrac{\partial u_y}{\partial y} = g_y - \dfrac{1}{\rho}\dfrac{\partial p}{\partial y} + \nu \left(\dfrac{\partial^2 u_y}{\partial x^2} + \dfrac{\partial^2 u_y}{\partial y^2} \right), \end{cases} \tag{5}$$

$$\frac{\partial^2 \bar{p}}{\partial x^2} + \frac{\partial^2 \bar{p}}{\partial y^2} = -\left\{ \left(\frac{\partial u_x}{\partial x} \right)^2 + 2 \left(\frac{\partial u_x}{\partial y} \right) \left(\frac{\partial u_y}{\partial x} \right) + \left(\frac{\partial u_y}{\partial y} \right)^2 \right\}. \tag{6}$$

In all the test cases presented in this paper, no turbulence model was incorporated into the RANS solution and surface tension effects were neglected.

Equations (5) and (6) were solved using the SIMPLE algorithm of FDM. The main idea of this method is applying the splitting technique to the solution. The first step is prediction of the velocity field integrating Equation (5): the explicit scheme is used to obtain values of the velocity components with values of pressure from the previous time step. In the second step, a correction of the pressure field is computed using Equation (6), which then corrects velocity to satisfy the zero divergence condition (4).

In order to determine the free surface location, the flow domain was defined using the Marker and Cell (MAC) method [9].

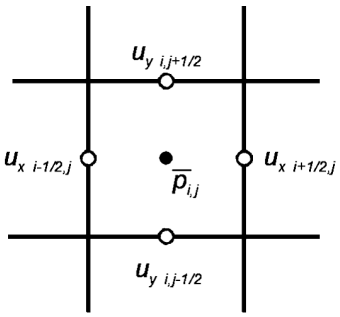

Figure 1. Cell specification for Euler staggered grid

In order to integrate the RANS system (5) and the Poisson Equation (6) in space with FDM, the two-dimensional domain x–y was discretized into a set of computational cells using the Euler staggered grid. In each cell, variables u_x, u_y and p were located in different positions (Figure 1). There were four types of cells (Figure 2): full (F), boundary (B), surface (S) and empty (E), depending on the location of cells and fluid inside the computational domain.

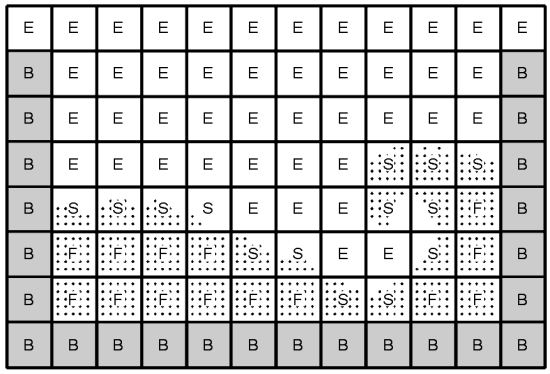

Figure 2. Discretization of the two-dimensional calculation domain (cells notations follow the MAC method)

Velocities were specified at the cells' interfaces, while pressure was specified at their center-points. RANS Equation (5) were approximated on a staggered grid by application of the two-step Lax-Wendroff Method (LWM2) [13], an approach ensuring accuracy of the second order. The pressure-correction Equation (6) was solved using the Successive Over-Relaxation (SOR) method [8]. The boundary conditions for these equations and their solution stability conditions had to be satisfied. The initial velocity field, $\boldsymbol{u}$, pressure $\bar{p}$ and the initial domain fill (initial position of the free surface) were specified by the initial conditions. The velocity terms were explicit, computed using known values, but the pressure term was implicit, based on the unknown pressure values at the next time step. The positions of markers in cells at a new time level was computed using the corrected velocity $\boldsymbol{u}$ and Newton's second law [8].

3. Numerical calculations and discussion of results

The mathematical model and numerical algorithm presented in the previous section were used to solve the dam-break flow (DBF) caused by an instantaneous rupture of the dam. The tests were carried out for a horizontal frictionless bottom. DBF simulations were carried out for four different values of depth downstream of the dam prior to the dam failure, h, (see Figure 3) equal to $0.0L$, $0.5L$, $1.0L$ and $1.5L$. For $h = 0.0$, the flow on a dry bottom downstream of the dam was considered, the problem being then equivalent to the water column collapse effect, discussed in [14] and [15], where the results of laboratory experiments carried out by Koshizuka *et al.* [16] were used to verify the numerical calculations and validate the model. The same model was used in this study; the domain geometry and the initial position of the water column and water in the downstream channel is presented in Figure 3.

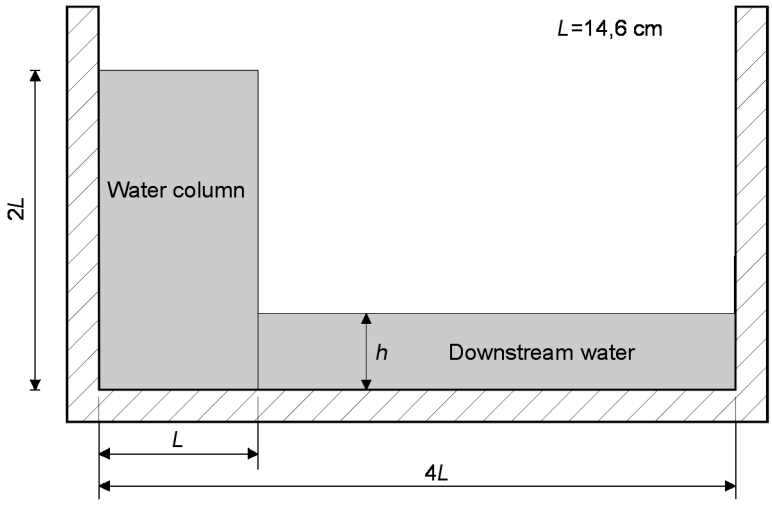

Figure 3. Domain geometry and initial shape of water column and water downstream

A RANS model numerical simulation was carried out with the following parameters: the number of cells equaled 1891 ($\Delta x = \Delta y = 0.973$), the number of particles depended on the depth of downstream water ($h = 0.0$, $h = 0.5L$, $h = 1.0L$ and

$h = 1.5L$) and varied from 1800 to 5850. A gravitation unit, $g_y = -9.806\,\mathrm{ms}^{-2}$, and a kinetic viscosity factor, $\nu = 10^3\,\mathrm{m}^2\mathrm{s}^{-1}$, were imposed. The viscous effect on the walls was neglected. The initial conditions of zero velocity and positions of marker particles were met. The position of particles – definition of the fill space – was connected with hydrostatic pressure distribution as an initial condition.

Exemplary results of computations according to the RANS model are presented in Figures from 4 to 7 (according to water depth in the downstream channel, h; particles' locations with velocity vectors – black points with arrows – and pressure distribution – shades of gray, see the legends). Only some of the markers used during simulation in the initial position are presented: after an instantaneous rupture of the dam (see subfigures (a)), after 0.2s and/or 0.3s and/or 0.4s and 0.5s. All the computations were performed for time of 0.5s.

The discrepancy between computations with the RANS and the SWE models is a result of different representation of pressure and velocity distribution along depth in both models. In SWE the pressure field is always hydrostatic and velocity is uniform along depth. Horizontal velocity and pressure distribution along depth computed with RANS model are presented for example simulations in Figures 8–10. The red line represents the mean velocity and hydrostatic distribution of pressure. During the first short-term period after water release, the pressure is non-linear and the horizontal velocity component is not constant along depth at the dam (discontinuity) cross-section ($x = L$ in Figure 11). This is noticeable in Figures 8–10, where the horizontal velocity and pressure distributions for the first moments after water release computed with the RANS model are presented. After this short-term effect, pressure and velocity respectively become almost hydrostatic and uniform. At other cross-sections ($x = 2L$ and $x = 3L$ in Figure 11) the pressure and velocity variation along depth is weaker and decays with time, especially when the depth of water in the downstream channel increases.

The evolution of pressure at the bottom of the dam's cross-section is presented in Figure 11; the computed pressure does not equal the hydrostatic pressure, especially at the beginning of the flow and when water splashes appear. However, the computed and hydrostatic pressures are approaching each other when the head of water increases and water splashes do not appear. Moreover, the evolution of pressure and depth fit well for other cross-sections, which means that non-linear pressure distribution is insignificant at these locations.

The presented results confirm that the non-linear pressure distributions and the non-uniform horizontal velocity variation near the flow discontinuity are short-term effects decaying with time, especially when the head of water is increased. This means that these short-term effects can be neglected as inessential for the simulated flow problem causing no damage to long-term simulations. Thus SWE can be used to describe rapidly varied flows for most of the practical water engineering problems where local effects occur but their inner structure can be neglected. The presented method can be applied where strong deformation, splashing or rapidly varied free surface occur.

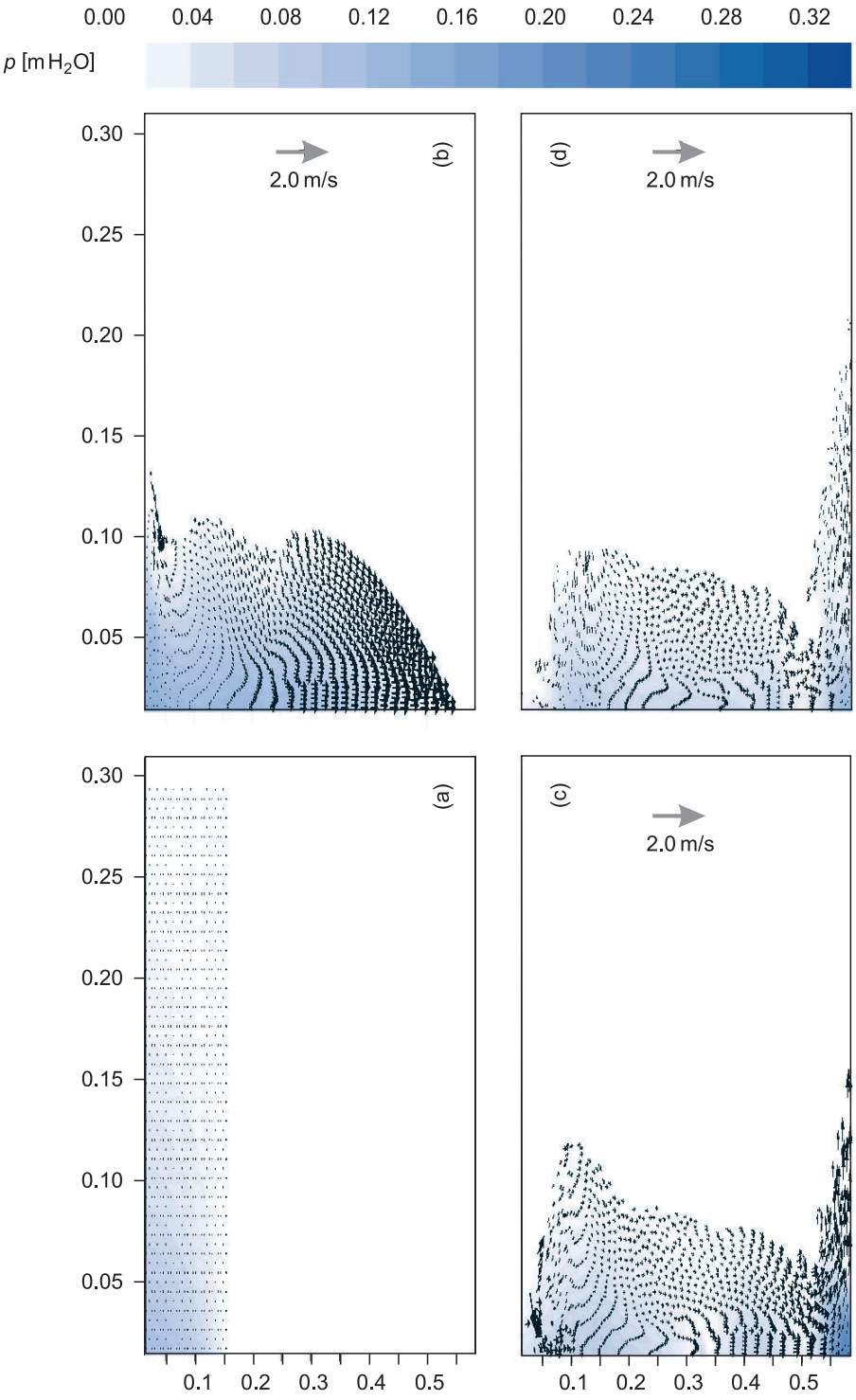

Figure 4. The calculated results of DBF for downstream water $h = 0.0$ after (a) $t = 0.0$s, (b) $t = 0.3$s, (c) $t = 0.4$s, (d) $t = 0.5$s of simulation

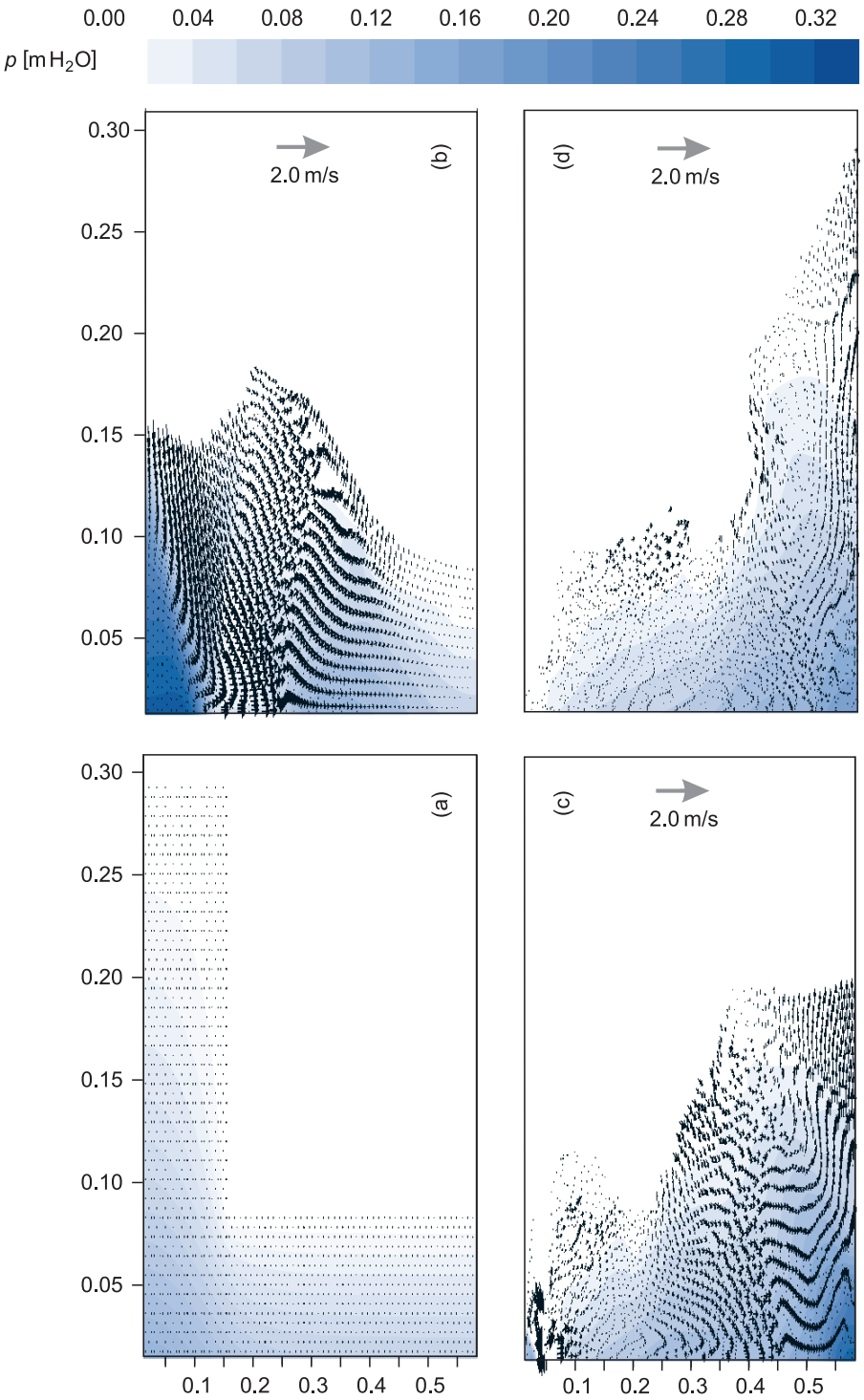

Figure 5. The calculated results of DBF for downstream water $h = 0.5L$ after (a) $t = 0.0$s, (b) $t = 0.2$s, (c) $t = 0.4$s, (d) $t = 0.5$s of simulation

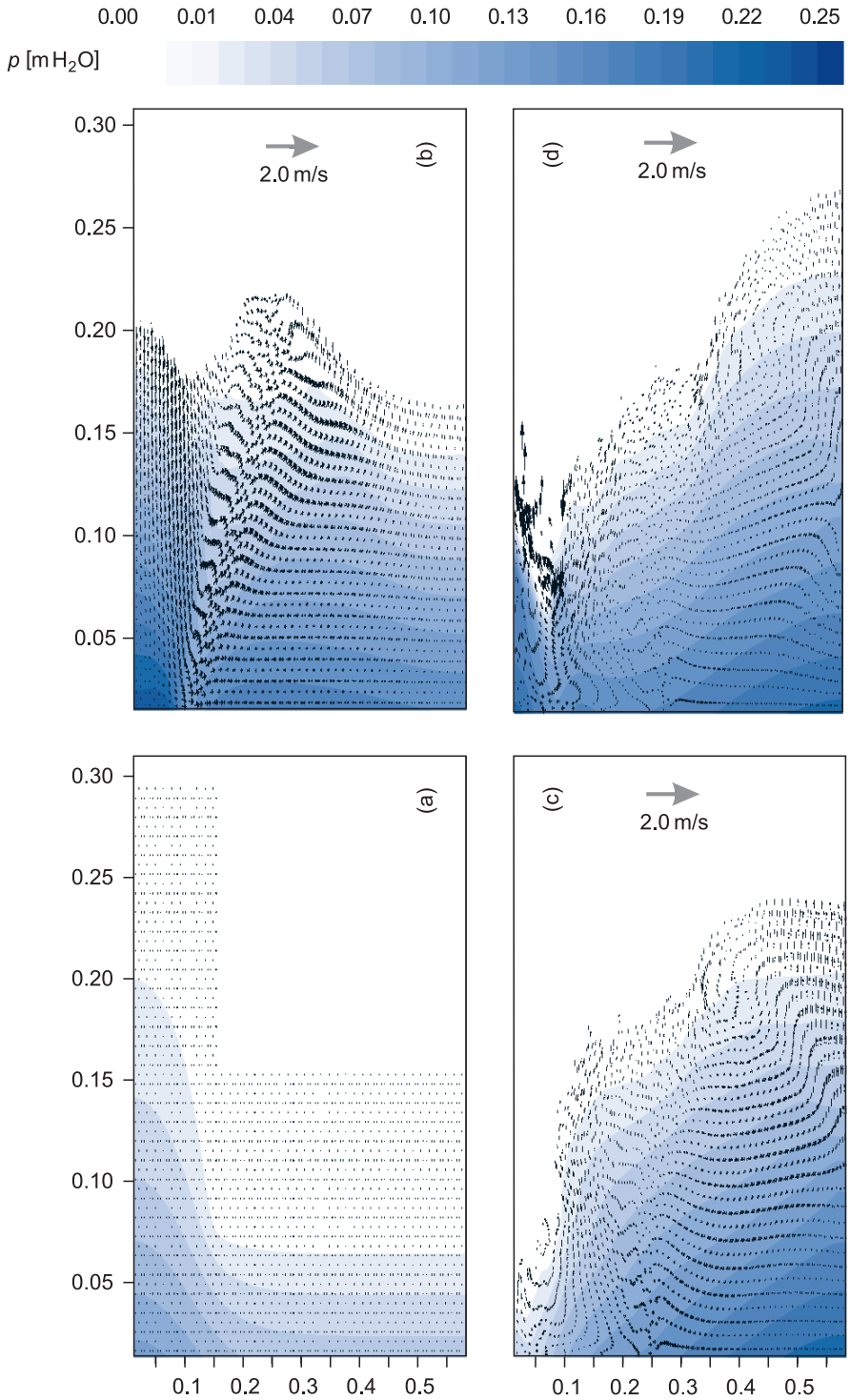

Figure 6. The calculated results of DBF for downstream water $h = 1.0L$ after (a) $t = 0.0$s, (b) $t = 0.2$s, (c) $t = 0.4$s, (d) $t = 0.5$s of simulation

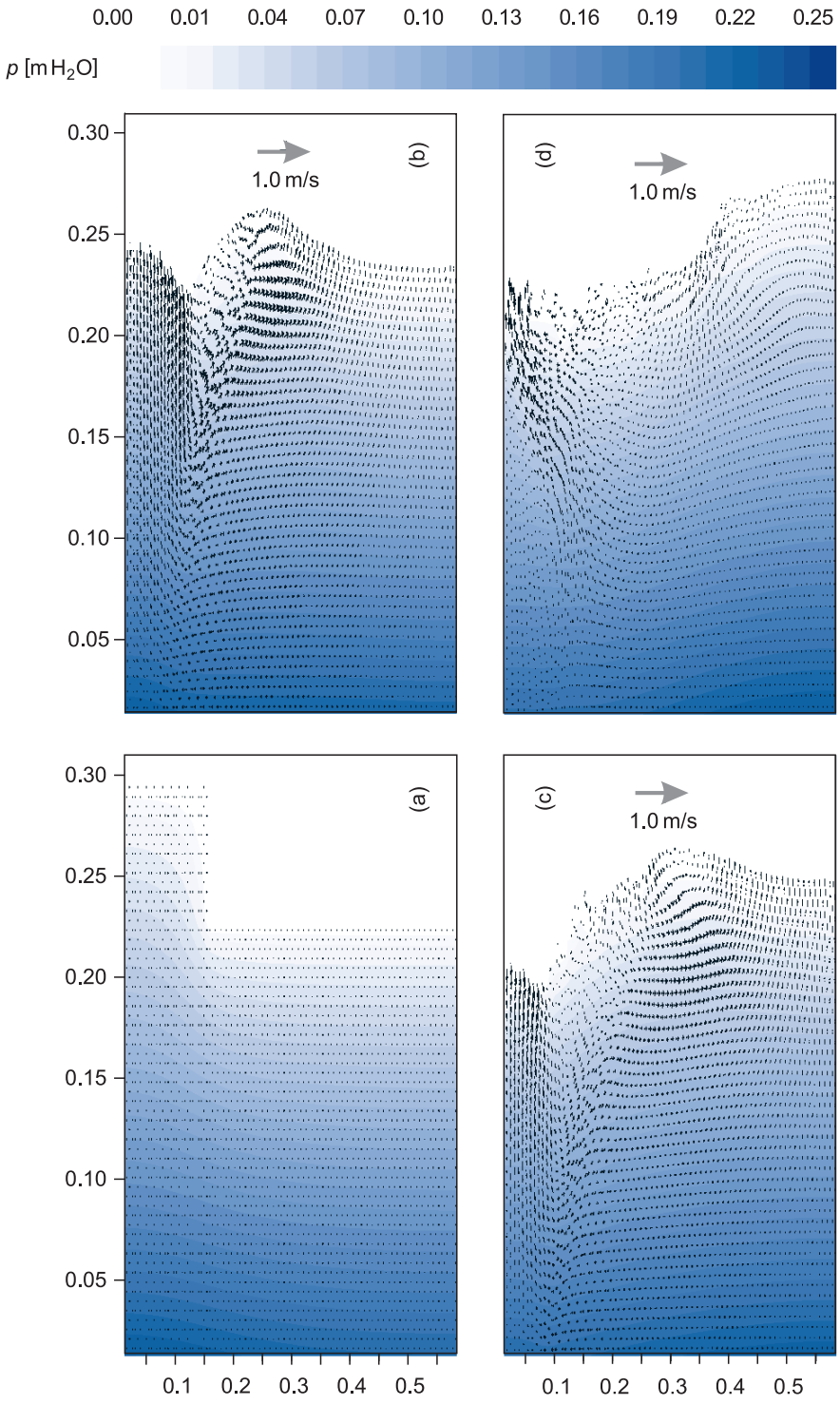

Figure 7. The calculated results of DBF for downstream water $h = 1.5L$ after (a) $t = 0.0$s, (b) $t = 0.2$s, (c) $t = 0.3$s, (d) $t = 0.5$s of simulation

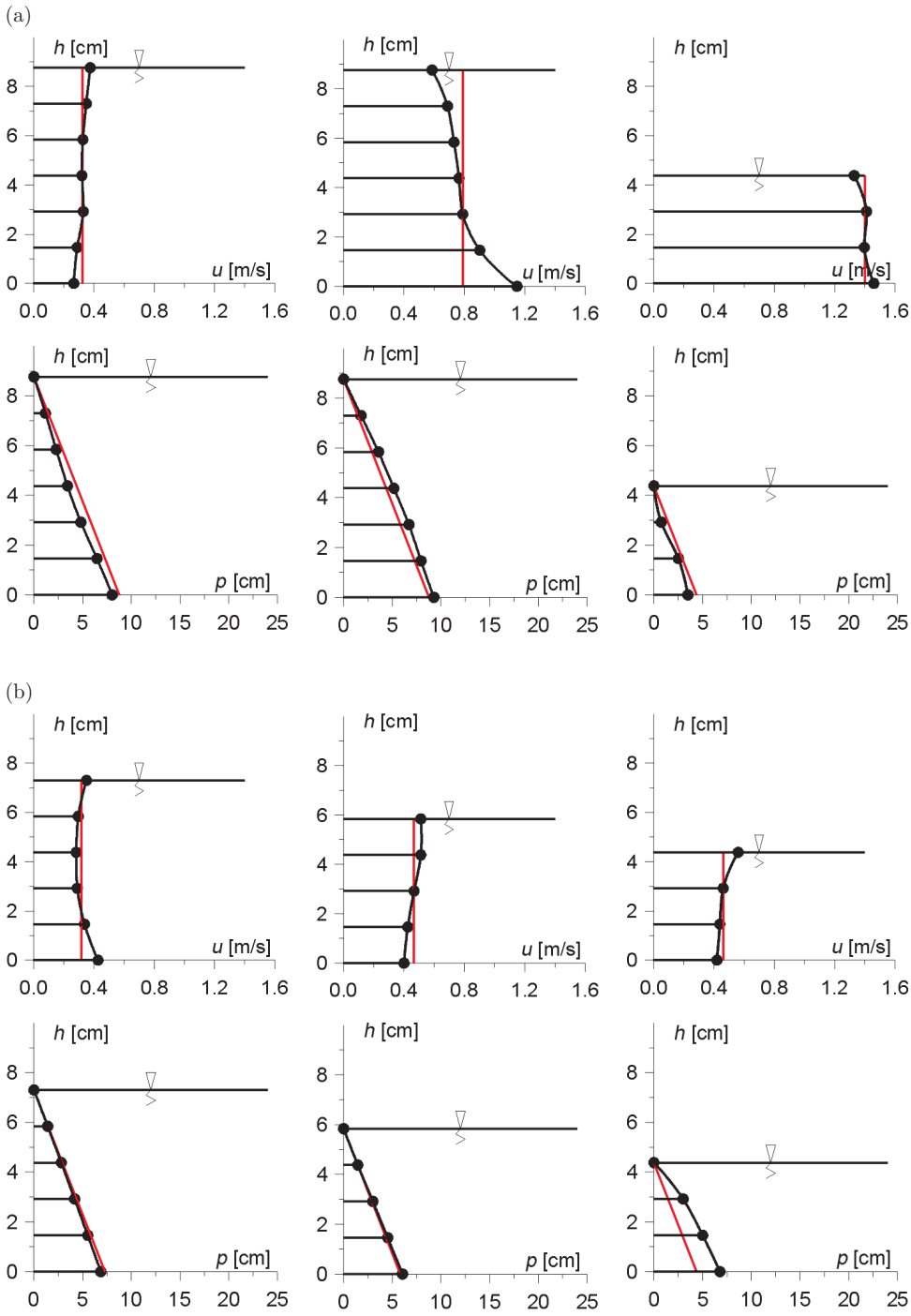

Figure 8. Horizontal velocity and pressure distribution along depth computed with the RANS model at selected cross-sections for $h = 0.0$ and: (a) $t = 0.3$s, (b) $t = 0.5$s; $x = L$, $x = 2L$ and $x = 3L$ for left, middle and right panels, respectively (red line marks the mean velocity and hydrostatic distribution of pressure)

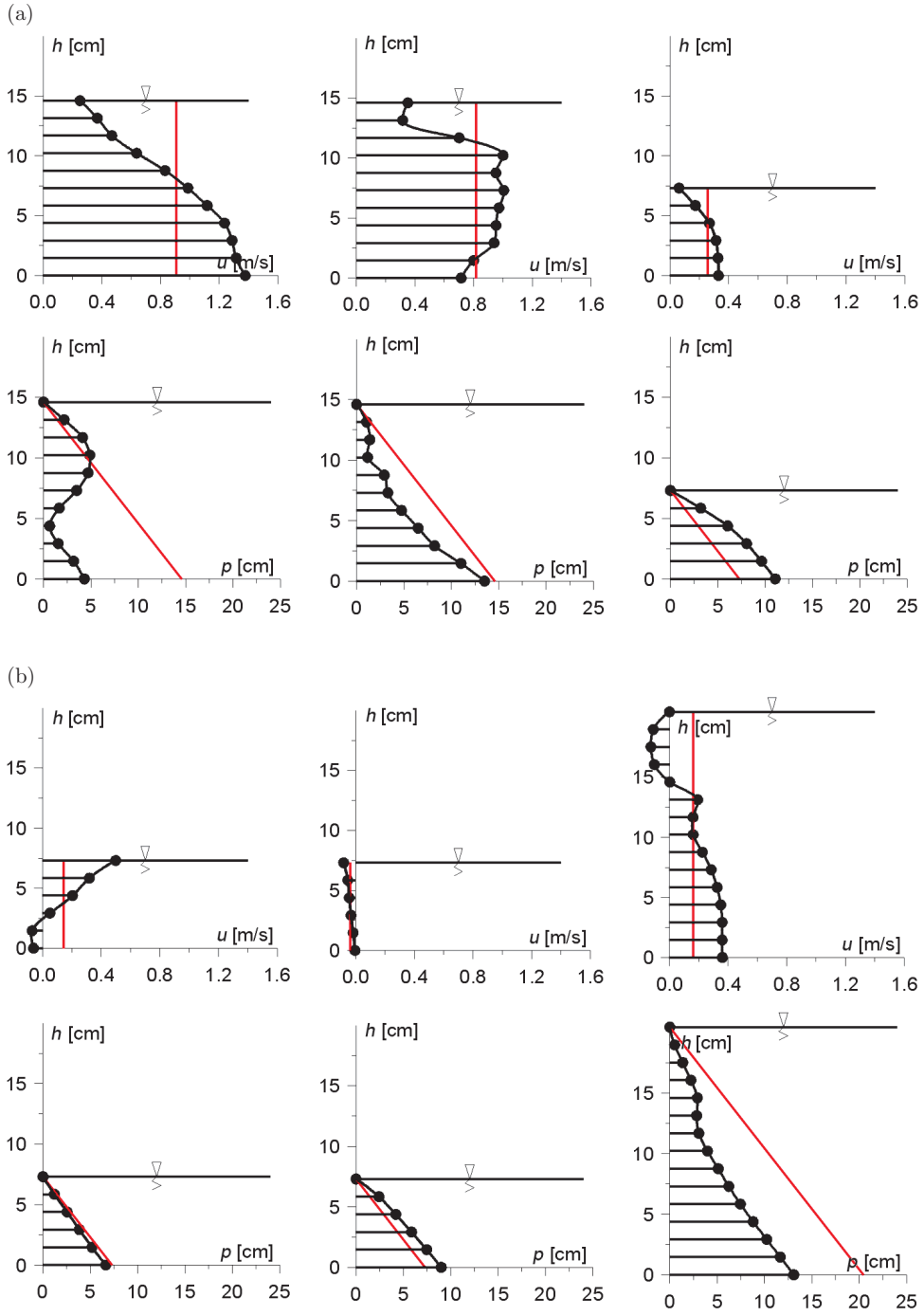

Figure 9. Horizontal velocity and pressure distribution along depth computed with the RANS model at selected cross-sections for $h = 0.5L$ and (a) $t = 0.2$s, (b) $t = 0.5$s; $x = L$, $x = 2L$ and $x = 3L$ for left, middle and right panels, respectively (red line marks the mean velocity and hydrostatic distribution of pressure)

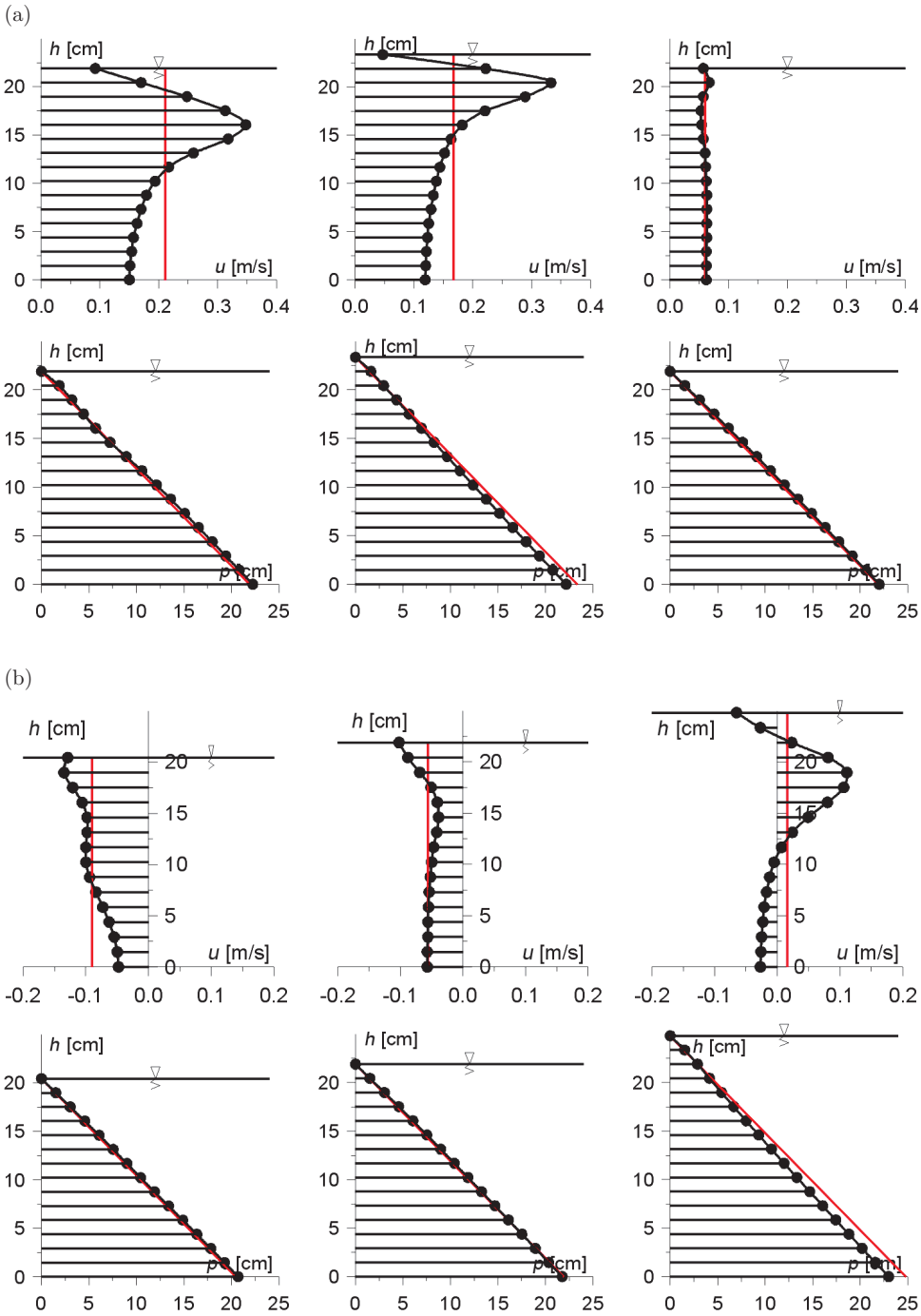

Figure 10. Horizontal velocity and pressure distribution along depth computed with the RANS model at selected cross-sections for $h = 1.5L$ and (a) $t = 0.2$s, (b) $t = 0.5$s; $x = L$, $x = 2L$ and $x = 3L$ for left, middle and right panels, respectively (red line marks the mean velocity and hydrostatic distribution of pressure)

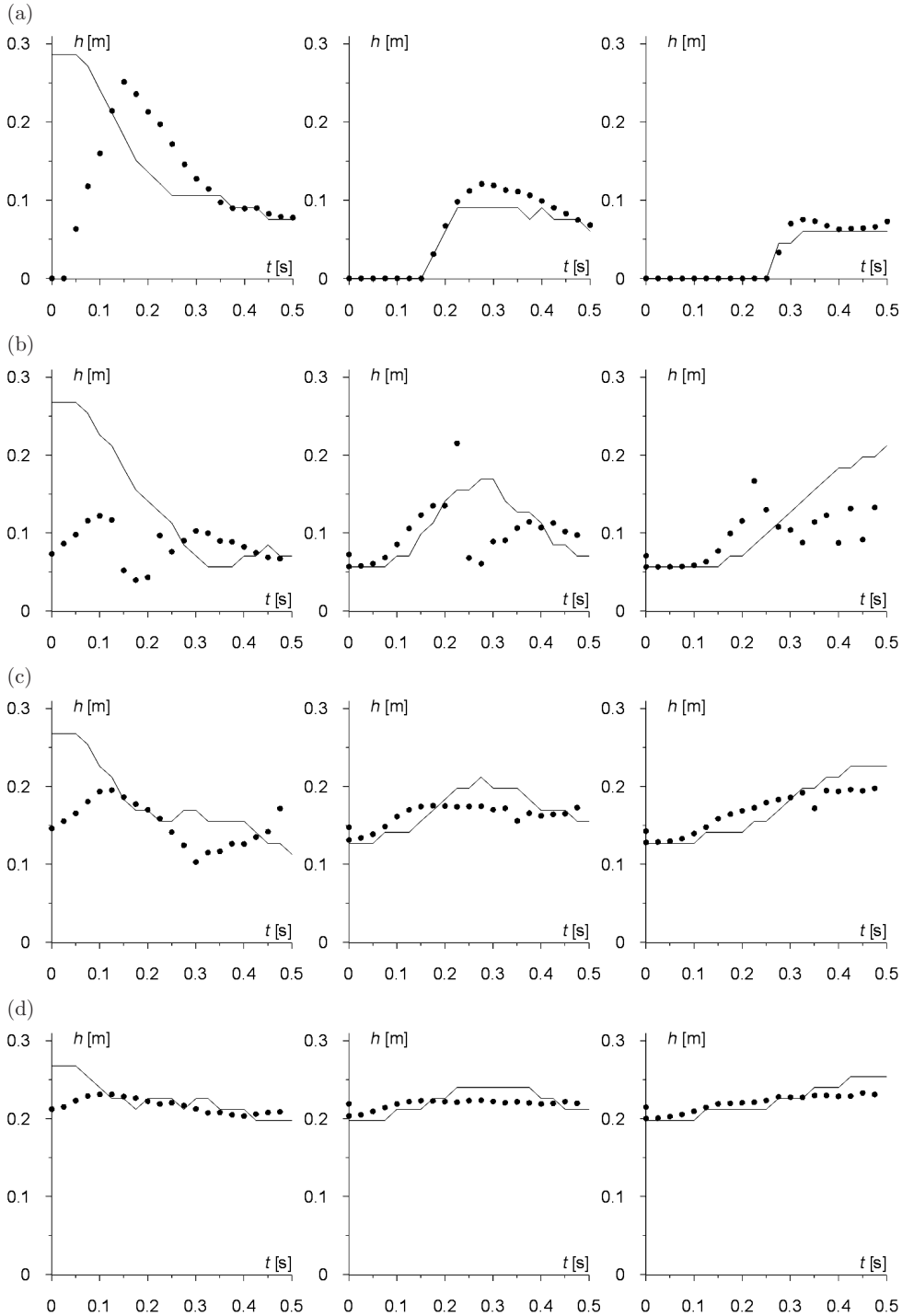

Figure 11. Pressure (•) and depth (–) evolution for
(a) $h = 0.0$, (b) $h = 0.5L$, (c) $h = 1.0L$ and (d) $h = 1.5L$;
$x = L$, $x = 2L$ and $x = 3L$ for left, middle and right panels, respectively

4. Conclusions

A rapidly varied open channel flow due to the dam-break effect has been analyzed in the paper. It has been established that the pressure distribution is non-hydrostatic immediately after the dam failure. The analysis was based on numerical investigations of the water column collapse problem on dry and wet bed (with various values of depth in the downstream channel). The focus has been on the time evolution of the flow's depth at the dam site and the evolution of pressure distribution towards a hydrostatic state. A mathematical model of RANS equations was used – to calculate the evolution of flow parameters.

It can be concluded that SWE models (assuming hydrostatic pressure and uniform velocity distribution along the water depth) do not offer an adequate description of the flow near local hydraulic effects (*i.e.* steep wave fronts, hydraulic jumps, water splashes, *etc.*). Better simulation results for short-term problems can be obtained using RANS equations, but that model is quite complex to use. Therefore, SWE equations still remain the main mathematical model of open-channel rapidly varied flows, ensuring sufficiently good simulation results for typical long-term engineering problems where the inner structure of local hydraulic effects and the short-term pressure and velocity distribution evolution can be neglected. The RANS model should be applied where strong deformation, splashing or rapidly varied free surface occur.

References

[1] Valiani A, Caleffi V and Zanni A 2002 *J. Hydraulic Engng* **128** (5) 460
[2] Szydłowski M 2005 *Archives of Hydro-Engineering and Environmental Mechanics*, Gdansk, **52** (4) 321
[3] Sawicki J 1998 *Free Surface Flows*, PWN, Warsaw (in Polish)
[4] Fletcher C A J 1991 *Computational Techniques for Fluid Dynamics: 1. Fundamental and General Techniques*, Springer-Verlag, Berlin
[5] Anderson J D 1995 *Computational Fluid Dynamics*, McGraw-Hill Inc, New York
[6] Tannehill J C and Anderson D A 1984 *Computational Fluid Mechanics and Heat Transfer,* Series in Computational and Physical Processes in Mechanics and Thermal Sciences, McGraw-Hill Book Company, New York
[7] Patankar S V 1980 *Numerical Heat Transfer and Fluid Flow*, McGraw-Hill Inc., New York
[8] Ferziger J H and Peric M 2002 *Computational Methods for Fluid Dynamics*, Springer
[9] Harlow F H and Welch J E 1965 *Physics of Fluids* **8** (12) 2182
[10] Maronnier V, Picasso M and Rappaz J 1999 *J. Comput. Phys.* **155** 439
[11] Mohapatra P K, Eswaran V and Bhallamudi S M 1999 *J. Hydraulic Engng* **25** (2) 183
[12] Zwart P J, Raithby G D and Raw M J 1999 *J. Comput. Phys.* **154** 497
[13] LeVeque R J 2002 *Finite Volume Method for Hyperbolic Problems*, Cambridge University Press, New York
[14] Zima P 2005 *Proc. Water Management and Hydraulic Engineering, 9th Int. Symposium* (Nachtnebel H P and Jugovic C J, Eds), Vienna, BOKU, Univ. Natural Resour. a. Appl. Sci., pp. 455–462
[15] Szydłowski M and Zima P 2006 *Archives of Hydro-Engineering and Environmental Mechanics*, Gdansk, **53** (4) 295
[16] Koshizuka S, Tamako H and Oka Y 1995 *Comput. Fluid Dyn. J.* **4** (1) 29